Nucleolar Diameter and Microvascular Factors as Independent Predictors of Mortality from Malignant Melanoma of the Choroid and Ciliary Body

Rana'a T. Al-Jamal,[1] *Teemu Mäkitie,*[1] *and Tero Kivelä*[1,2]

Purpose. To determine whether nucleolar diameter and microvascular factors are independent predictors of mortality in malignant uveal melanoma of the choroid and ciliary body.

Method. A population-based retrospective cohort study was conducted of melanoma-specific and all-cause mortality in 167 consecutive patients who had an eye enucleated because of choroidal and ciliary body melanoma from 1972 through 1981. The largest nucleoli were measured from digital photographs of silver-stained tumors along a central 5-mm-wide linear field parallel to the base of the tumor. The mean of the 10 largest nucleoli (MLN) was calculated. Microvascular loops and networks and microvascular density (MVD) were assessed. Kaplan-Meier and Cox regression analyses were performed. Associations between MLN and other variables were determined.

Results. The MLN could be determined in 126 (75%) melanomas. It ranged from 2.60 to 6.18 μm (median, 4.05). The association of large MLN with the presence of epithelioid cells ($P = 0.017$) and high MVD ($P = 0.0053$) was statistically significant. MLN was not significantly associated with tumor diameter and microvascular loops and networks. The 10-year melanoma-specific survival decreased with MLN (0.74, 0.60, and 0.42, arranged in tertiles; $P = 0.0060$), presence of loops and networks ($P = 0.0001$), and increasing MVD ($P = 0.0001$). By Cox regression, MLN was an independent predictor of survival, when adjusting in turn for presence of epithelioid cells, loops and networks, and MVD. In multivariate models with MVD, the independent prognostic information carried by MLN decreased, but the model as a whole was a better predictor of survival. The magnitude of this effect depended on whether MLN was modeled as a continuous or categorical variable.

Conclusions. In this population-based data set, MLN and microvascular loops and networks were unrelated, independent predictors of survival. MLN and MVD were found to be partially interrelated. Multivariate models that included MVD in addition to MLN fitted better with observed melanoma-specific survival than models that excluded MVD. (*Invest Ophthalmol Vis Sci.* 2003;44:2381–2389) DOI:10.1167/iovs.02-1215

During the past decade, two main lines of research have sought to derive an accurate prognosis for patients with uveal melanoma. One has emphasized characteristics of tumor cells, particularly their nucleoli[1–17] and markers of proliferation,[13,15,18–21] and the other characteristics of tumor blood vessels.[9,10,15,22–34] Of several morphometric measurements, the mean diameter of the 10 largest nucleoli (MLN) has become the most widely applied.[2,4–11,15,17] A large MLN has consistently been associated with a high chance of dying of uveal melanoma.[2,5–7,10,15,17] Many methods have been used to stain[4,11] and sample the largest nucleoli,[2,4,5,8,11,17] and no agreement has yet been reached as to which combination is the best.

Regarding microvascular factors, the morphologic arrangement, or pattern, of microvessels and associated extracellular matrix, identified by periodic acid–Schiff staining,[9,10,15,22–25,27,28,30,32–34] and microvascular density (MVD), identified by antibodies to endothelial cells[26–29,31,35] have been addressed. Certain microvascular patterns—parallel with cross-linking, arcs, arcs with branching, loops and networks,[9,10,15,22,24,25,27,30,32,34,35]—and high MVD[26,28,31,35] have been associated with a high mortality rate in persons with uveal melanoma. In fact, provisional evidence has been provided that melanoma cells in addition to blood vessels may contribute to both measures.[33,35,36]

Whereas microvascular patterns and MVD, when the latter is determined from areas of densest vascularization, independently contribute to prognosis of uveal melanoma,[31,35] the relative contribution of MLN and microvascular factors is debated. One study suggested that loops and networks rather than MLN are prognostic.[8] In contrast, others observed that MLN had a stronger association with mortality than loops,[10] or that networks and MLN were about equally associated with prognosis, although less strongly than proliferation indices.[15] Possible association between and the relative prognostic relevance of MVD and MLN have never been evaluated.

Our goal was to clarify the relationship between MLN and microvascular factors in malignant uveal melanoma of the choroid and ciliary body and to determine how this relationship affects prognosis and survival, so as to improve understanding of this tumor. A special motivation was that the number of uveal melanomas that are available for histopathology is again likely to increase in the near future because of improved techniques for transscleral resection[37–39] and the hope that such procedures would be more efficient than irradiation in preserving vision,[39] especially when the tumor is medium sized.

From the [1]Ophthalmic Pathology Laboratory and the [2]Oncology Service, Department of Ophthalmology, Helsinki University Central Hospital, Helsinki, Finland.

Supported by grants from the Finnish Medical Research Fund, Grant TYH 1217 from the Helsinki University Central Hospital Research Fund, and the Eye Foundation, Helsinki, Finland. RTA-J is a stipendiate of the Ministry of Health, Amman, Jordan; the World Health Organization, Amman, Jordan; and Center for International Mobility, Helsinki, Finland.

Submitted for publication November 26, 2002; revised January 23, 2003; accepted January 30, 2003.

Disclosure: **R.T. Al-Jamal**, None; **T. Mäkitie**, None; **T. Kivelä**, None

The publication costs of this article were defrayed in part by page charge payment. This article must therefore be marked "*advertisement*" in accordance with 18 U.S.C. §1734 solely to indicate this fact.

Corresponding author: Tero Kivelä, Ophthalmic Pathology Laboratory, Department of Ophthalmology, Helsinki University Central Hospital, Haartmaninkatu 4 C, PL 220, FIN-00029 HUS, Helsinki, Finland; tero.kivela@helsinki.fi.

Patients and Methods

Study Design

The primary objective was to determine whether nucleolar size and microvascular factors are independently associated with survival of patients with uveal melanoma. The secondary purpose was to study the interrelationship between MLN, microvascular loops and networks, and MVD.

Study Population and Exclusion Criteria

We studied a cross-sectional, population-based cohort of 167 patients with uveal melanoma, previously used for analysis of microvascular loops and networks. The cause of death had been validated by reviewing all patient charts relating to malignant tumors and death, cross-checking with the Finnish Population and Cancer Registries, and by acquiring all histopathological material available from primary tumors, metastases, and second cancers.[31,32,40]

The 167 consecutive patients, who had a choroidal or ciliary body melanoma enucleated between 1972 and 1981, were verified from the records of the Ophthalmic Pathology Laboratory, Helsinki University Central Hospital. During that time, enucleation was the only treatment available for uveal melanoma, and all removed eyes were submitted to this laboratory.

Complete follow-up data, with a median follow-up time of 25 years (range, 20–29) for those still alive, were available for 166 of the 167 patients. The diagnoses of all 9 secondary cancers and 49 of 53 specimens of metastatic uveal melanoma were confirmed by immunohistochemistry.[31,32,40] The study followed tenets of the Declaration of Helsinki and was approved by local review board.

Assessment of Nucleolar Size

Both hematoxylin-eosin staining[2,4–8,10,11,15] and silver staining,[11,17] originally designed for labeling nucleolar organizing regions, have been used to identify nucleoli for measurement. The silver stain provides high contrast between nucleoli and other structures, allowing accurate discrimination of nucleoli.[11,17] A comparative study found that measurements from silver-stained slides were easier to make and provided better prognosis than those from hematoxylin-eosin slides.[17] The most frequent field selection for sampling has been a 5-mm-long linear strip from the center of the melanoma. Linear sampling was recently reported to be comparable to scanning nucleoli from the entire tumor section in predicting outcome.[17] For these reasons, we chose silver staining and linear sampling for the present study.

Sections were cut at 5 μm on chromium-gelatin–treated glass slides[41] and randomly coded. The code was broken only after all MLN measurements had been obtained. After deparaffinization, the sections were bleached with 0.25% (wt/vol) potassium permanganate for 1 hour and 5.0% (wt/vol) oxalic acid in distilled water for 5 minutes. One-step silver staining was performed using two solutions[11,17]: first, 2.0% (wt/vol) gelatin (Bacto Gelatin; Difco Laboratories, Detroit, MI) and 0.88% (vol/vol) formic acid in distilled water; second, 50% (wt/vol) silver nitrate in distilled water. The solutions were mixed 1:2 in the dark and poured into a dish to cover the specimens for 30 minutes. The sections were washed in distilled water and dehydrated, and coverslips were mounted (Mountex; Histolab Products AB, Göteborg, Sweden).

Each slide was examined under a light microscope (BH-2; Olympus, Tokyo, Japan) at 20× magnification to orient the central longest axis of the tumor parallel to tumor base for digital photography (DP-10; Olympus). A photograph under low magnification was first taken for documentation of orientation. A series of color photographs under 400× optical magnification were obtained to image the nucleoli along this axis. A 5-mm strip was photographed, divided into 25 slightly overlapping images (resolution, 1280 × 1024 pixels, image area 218 × 175 μm). In case the tumor was less than 5 mm by largest basal diameter (LBD), the entire central axis of the tumor was photographed.

From each of the 25 photographs, the largest nucleoli were measured by image-analysis software (Olympus DP-10 Soft, ver. 3.0; Soft Imaging System GmbH, Münster, Germany). A strip one screen high at 300% digital magnification (final magnification on screen, ×4700; corresponding to 41 μm) was scanned from the top of each photograph. Measurements were taken along the longest axis of the nucleoli. The number of nucleoli measured was one to five per image (13 to 80 per

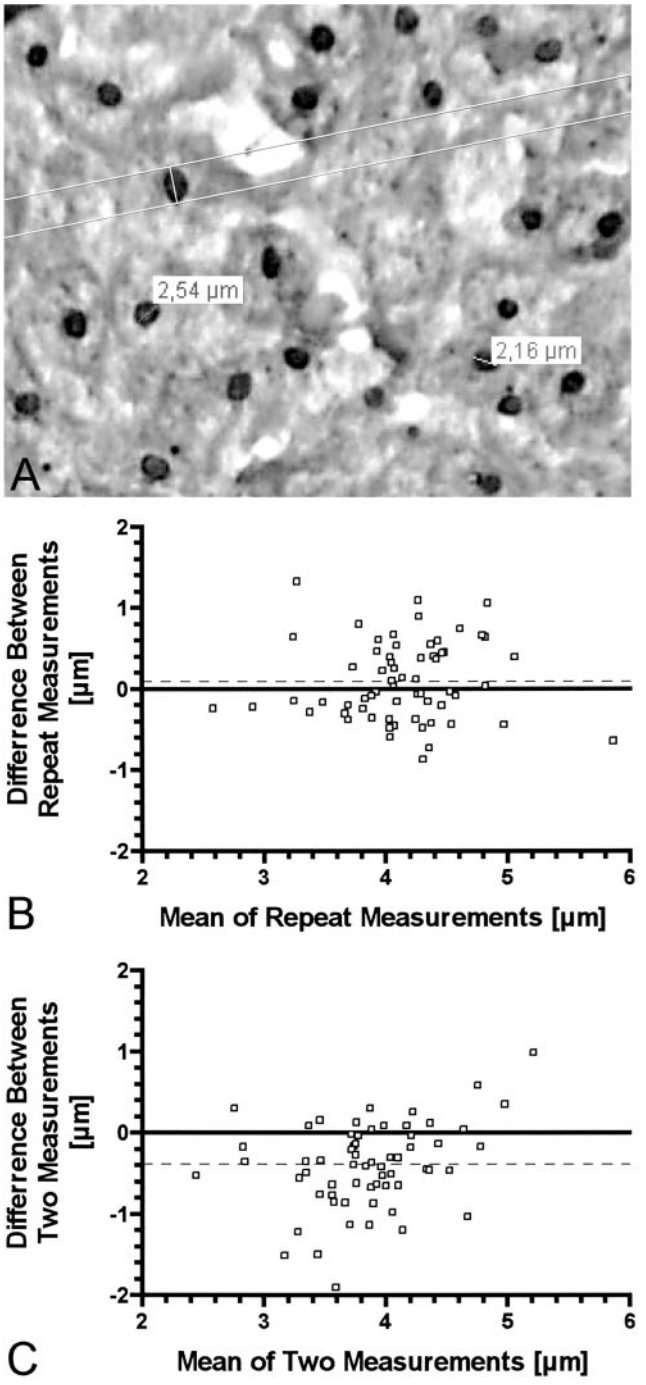

Figure 1. Assessment of MLN in choroidal and ciliary body melanoma. (**A**) The longest diameter of silver-stained nucleoli was measured from computer screen at 4700× magnification with a digital caliper (*white lines*). Screen height corresponded to 41 μm, and the field scanned from each photograph was several screen widths wide. (**B**) Plot of intraobserver agreement between repeated measurements and (**C**) interobserver agreement between two observers in assessing MLN from a randomly drawn subset of 63 melanomas. *Dashed lines*: mean difference between measurements.

TABLE 1. MLN of 126 Choroidal and Ciliary Body Melanomas Studied Compared With Literature Data

	MLN		Methodology			
Source	**Mean**	**Range**	**Staining**	**Field**	**Measurement**	**Data Set**
Present study/observer I	4.06	2.60–6.18	Silver§	5 mm parallel to tumor base through center	Largest diameter	Consecutive
Present study/observer II*	3.71	2.18–6.61	Silver§	5 mm parallel to tumor base through center	Largest diameter	Consecutive
Moshari/AgNOR[17]	3.13	1.10–5.50	Silver§	Entire tumor area	Largest diameter	Selected‖¶
Moshari and McLean/H&E[17]	2.84	2.00–5.20	HE	Entire tumor area	Largest diameter	Selected‖¶
Moshari and McLean/McCurdy[17]	2.69	1.03–4.84	HE	5 mm parallel to longest axis through center	Horizontal diameter	Selected‖¶
Seregard et al.[15]	3.34†	2.07–5.53	HE	5 mm through tumor	Horizontal diameter	Selected‖
Pe'er et al./Observer I[8]	3.76	2.31–6.62‡	HE	5 mm parallel to longest axis through center	Largest diameter	Consecutive
Pe'er et al./Observer II[8]	3.96	2.76–8.79	HE	5 mm parallel to longest axis through center	Largest diameter	Consecutive
Sørensen et al.[7]	2.77	1.61–4.85	HE§	5 mm parallel to longest axis through center	Horizontal diameter	Selected‖¶
Sørensen et al.[6]	3.06	2.20–4.23	HE	5 mm parallel to longest axis through center	Horizontal diameter	Consecutive

* Based on a randomly drawn subset of 63 tumors.
† Median.
‡ Excluding one outlier of 11.2 μm.
§ Mentions bleaching of melanin.
‖ Excluded patients who survived less than 9–10 years from treatment without metastasis.
¶ Included 50% of patients who died of melanoma and 50% who survived without metastasis

section; total area, 0.205 mm^2). The mean of the 10 largest nucleoli was calculated.

The images from a randomly drawn set of 63 (50%) slides were remeasured after 6 weeks by the same observer, and a second observer also graded the same images to asses intraobserver and interobserver variability, respectively.

Assessment of Microvascular Factors

Closed microvascular loops and microvascular networks, consisting of at least three back-to-back loops, were identified according to Folberg et al.[22,24] from sections bleached with potassium permanganate and oxalic acid and stained with periodic acid–Schiff without counterstain.[31,32] They were viewed under a green filter (Wratten No. 58; Eastman Kodak, Rochester, NY). Loops of all sizes were taken into account.

Microvessels were identified with the monoclonal antibody QBEND/10 to the CD34 epitope of endothelial cells (lot 121202; Novocastra Laboratories, Newcastle-upon-Tyne, UK; diluted 1:25).[42] They were counted at 400× magnification from the most highly vascularized area (hot spot), using an eyepiece with an etched graticule corresponding to 0.313 mm^2 (WK 10x/20L-H; Olympus).[31] Any immunolabeled element, clearly separate from adjacent ones and totally inside the graticule or touching its top or left border, was counted as a microvessel.[28]

Statistical Analysis

Analyses were performed on computer (Stata, ver. 7.0; Stata Co., College Station, TX). Intraobserver agreement in measuring MLN was assessed by plotting the difference between the measurements against their mean and by calculating the mean difference with 95% confidence limits.[43] Interobserver reproducibility was assessed similarly.

To compare MLN in various types of uveal melanoma, the groups were compared with the nonparametric Kruskal-Wallis test. Nonparametric test for trend, which is an extension of Wilcoxon rank sum test,[44] was used if the groups were ordered. The association between MLN and other continuous variables was analyzed by Spearman's rank correlation. All tests used were two tailed.

Univariate analysis of survival time data were based on the Kaplan-Meier product-limit method without taking competing risks into account.[45,46] Patients judged to have died of causes other than uveal melanoma were censored at the time of death. Minimum sample size was calculated on the basis of a previous consecutive series, which reported the cumulative 10-year probability of survival to be 0.69 and 0.22 for patients who had a melanoma in which MLN was lower and higher than the median, respectively, corresponding to a survival difference of 0.47.[6] Power analysis indicated that to detect a similar difference as significant with a power of 80%, the study should have a minimum of 58 patients (Power and Precision, ver. 2.0; Biostat, Englewood, NJ).

Cell type and tumor location were collapsed into two categories according to the presence of epithelioid cells (spindle, nonspindle)[41] and ciliary body involvement (no, yes), respectively. Microvascular loops and networks were analyzed as a three-category variable that considered networks to be an advanced stage of loops (no loops, loops without networks, networks).[22,32] LBD, MVD, and MLN were divided into tertiles.

Cox proportional hazards regression was used to adjust survival time data for the effect of other prognostic factors.[45] LBD and MVD were modeled as continuous variables, and MLN alternatively as divided in tertiles to assess robustness of results. MVD was square-root transformed to obtain normal distribution.[28,31] Independent variables were allowed in the model if $P < 0.10$, and different models were compared with the likelihood ratio test.[46] The number of variables was restricted to four, based on a rule to have at least 15 to 20 events for each additional variable.[45] The regression coefficients and hazard ratios (HR) with 95% confidence intervals (CI) were calculated. The assumption of proportional hazards was tested by the method of Therneau and Grambsch.[47]

RESULTS

Mean Diameter of the 10 Largest Nucleoli

Nucleoli were reliably identified using the silver staining method in 126 (75%) of the 167 slides (Fig. 1A). The remaining 41 specimens were technically not satisfactory, because of loss

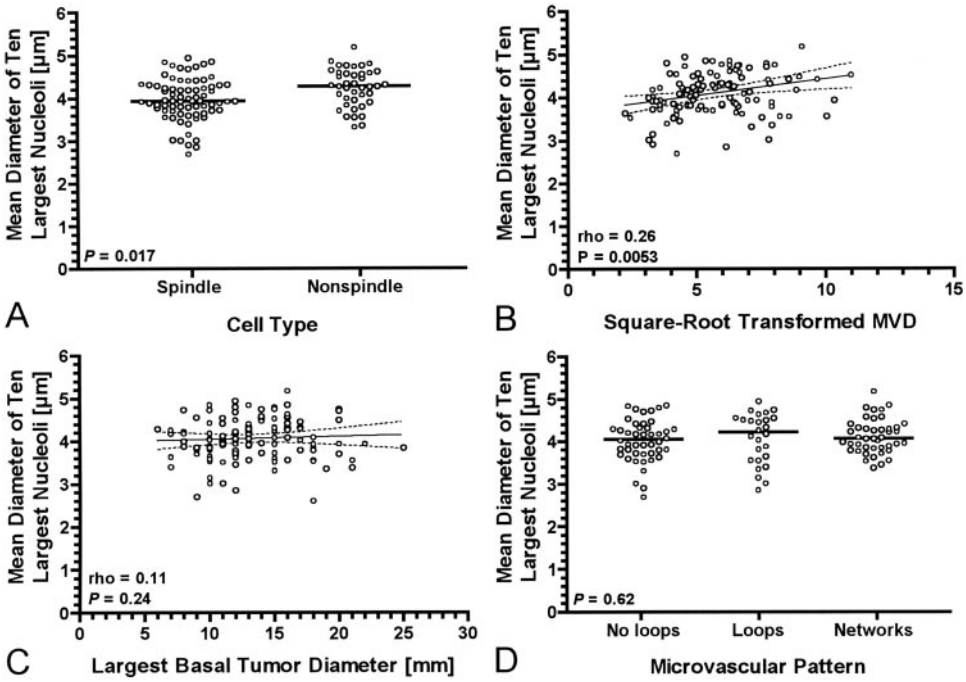

FIGURE 2. Scattergrams of MLN against the presence of epithelioid cells (**A**), square-root–transformed MVD obtained from the area of highest vascularization after staining with antibodies against CD34 epitope (**B**), tumor LBD (**C**), and presence of microvascular loops and networks (**D**) in choroidal and ciliary body melanoma. Note considerable overlap in MLN between categories. (**A**, **D**, *horizontal bars*) median; (**C**, **D**, *lines*) linear regressions with 95% confidence limits.

of tissue, because artifacts made it difficult to recognize the nucleoli in some heavily pigmented tumors or because the tumor was very small. Likewise, microvascular factors were reliably determined from 134 (80%) specimens. MLN and microvascular factors were both available for 113 (68%) tumors.

The median MLN based on the 10 largest nucleoli per tumor was 4.05 μm (range, 2.60–6.18), and the mean was 4.06 $\pm$ 0.54 μm (SD). The mean and range were of the same order of that previously reported in studies using different methodologies (Table 1).

Intraobserver reproducibility in assessing MLN, evaluated by the mean difference between the repeated measurements, was +0.097 μm (95% CI, –0.025 to +0.22) on remeasurement (Fig. 1B). The corresponding mean interobserver difference between measurements was –0.38 μm (95% CI, –0.51 to –0.25; Fig. 1C). The latter difference seemed to be due in part to personal preference in positioning the caliper in relation to the border of the nucleolus, which generally was slightly blurred.

Association with Other Prognostic Variables

MLN was significantly larger if epithelioid cells were present than if the tumor consisted only of spindle cells (difference, 0.31 μm; $P = 0.017$, Kruskal-Wallis test; Fig. 2A), and it increased with increasing MVD ($P = 0.0053$, Spearman correlation; Fig. 2B). Nevertheless, notable overlap was observed between categories (Figs. 2A, 2B; Table 2). No significant association was observed between MLN and gender, involvement of the ciliary body, LBD ($P = 0.24$, Spearman correlation; Fig. 2C), tumor pigmentation, presence of tumor-infiltrating macrophages, and microvascular loops and networks ($P = 0.62$, nonparametric test for trend; Fig. 2D; Table 2).

Kaplan-Meier Analysis of Survival

At the end of follow-up, 26 (21%) of 126 patients were alive, 60 (48%) had died of metastatic uveal melanoma, 8 (6%) of a histopathologically verified second cancer, 31 (25%) of unrelated nonmalignant disease, and 1 of an unknown cause.

Both melanoma-specific and all-cause survival rates were significantly associated with MLN ($P = 0.0060$ and $P = 0.015$, respectively, log-rank test for trend; Figs. 3A, 3B). The 10-year Kaplan-Meier estimate for melanoma-specific survival was 0.74 (95% CI, 0.56–0.85) for small, 0.60 (95% CI, 0.44–0.74) for medium, and 0.42 (95% CI, 0.25–0.58) for large MLN.

Melanoma-specific survival was also associated with LBD ($P = 0.0007$, log-rank test for trend; Fig. 3C), the presence of epithelioid cells ($P < 0.0001$, log-rank test; Fig. 3D) and microvascular loops and networks ($P = 0.0001$, log-rank test for trend; Fig. 3E), and MVD ($P = 0.0001$; Fig. 3F). The Kaplan-Meier estimate for 10-year melanoma-specific survival was 0.80 (95% CI, 0.64–0.90) if no loops, 0.48 (95% CI, 0.27–0.67) if loops were present without networks, and 0.40 (95% CI, 0.25–0.55) if loops forming networks were present. The corresponding estimates according to tertiles of MVD were 0.86 (95% CI, 0.70–0.94), 0.50 (95% CI, 0.33–0.65), and 0.41 (95% CI, 0.24–0.57), respectively.

Cox Regression Analysis of Survival

By univariate analysis, MLN was significantly associated with melanoma-specific survival, whether modeled as a continuous variable (HR 1.82 for each micrometer increase; $P = 0.016$) or a categorical one (HR 1.57 for each category increase, by tertile; $P = 0.007$; Table 3).

The second observer who graded a subset of 63 tumors drew conclusions qualitatively and quantitatively similar to those of the first observer, based on the same set (hazard ratio, 2.0 vs. 1.6; Wald χ^2 5.29 vs. 4.80, $P = 0.021$ vs. 0.029, respectively). In addition, four of five of the bivariate associations reported for the entire data set of 126 patients (described later) were also identified by using data of either observer for the 63 patients.

The presence of ciliary body involvement; large LBD; presence of epithelioid cells, high grade of pigmentation; presence of microvascular loops and networks, as modeled by assuming networks to be an advanced stage of loops (HR 1.80 for each category increase; $P < 0.001$); and high MVD (HR 1.02 for each unit increase in square-root–transformed count; $P < 0.001$)

TABLE 2. MLN According to Clinicopathological Characteristics of 126 Choroidal and Ciliary Body Melanomas

Characteristic	MLN		*P*
	Median (Range)	Mean (SD)	
Gender			0.21*
Female	3.98 (2.60–6.18)	4.01 (0.56)	
Male	4.18 (2.70–5.18)	4.12 (0.49)	
Tumor location			0.44*
Choroid only	4.02 (2.60–6.18)	4.04 (0.55)	
Ciliary body involved	4.13 (2.91–4.95)	4.11 (0.51)	
Largest basal diameter (mm)			0.11*/0.23†
≤10	3.85 (2.70–4.86)	3.90 (0.50)	
>10–15	4.17 (2.86–6.18)	4.15 (0.53)	
>15	4.03 (2.60–5.18)	4.05 (0.56)	
Cell type			0.017*
Spindle	3.96 (2.70–6.18)	4.02 (0.56)	
Nonspindle	4.27 (3.32–5.18)	4.24 (0.45)	
Pigmentation			0.70*/0.84†
Weak	4.06 (2.86–6.19)	4.07 (0.64)	
Medium	4.06 (3.02–5.18)	4.10 (0.47)	
Strong	4.01 (2.70–4.86)	4.02 (0.53)	
Macrophages			0.89*/0.78†
Few	4.18 (2.86–5.18)	4.07 (0.51)	
Moderate	4.08 (3.02–4.86)	4.12 (0.46)	
Many	3.79 (2.60–4.54)	3.71 (0.52)	
Microvascular pattern			0.83*/0.62†
No loops	4.06 (2.70–6.18)	4.07 (0.59)	
Loops only	4.22 (2.86–4.95)	4.08 (0.60)	
Networks	4.06 (3.38–4.86)	4.12 (0.41)	
Microvascular density			0.0029*/0.017†
≤23 vessels	3.87 (2.70–4.95)	3.88 (0.49)	
24–42 vessels	4.27 (2.86–4.86)	4.23 (0.39)	
>42 vessels	4.15 (3.02–6.18)	4.19 (0.38)	

* Kruskal-Wallis test, two-tailed.
† Nonparametric test for trend, two-tailed.

were also significantly associated with melanoma-specific survival (Table 3).

MLN remained an independent predictor of prognosis, both as a continuous and categorical variable when adjusted in turn for the effect of ciliary body involvement, LBD, presence of epithelioid cells, and microvascular loops and networks (Table 3). When adjusted for MVD, it was of borderline significance as a continuous variable ($P = 0.11$; Table 3). Of the five bivariate models tested, those that combined MLN with cell type and MVD best predicted melanoma-specific survival, whether MLN was modeled as a continuous or categorical variable (e.g., model 3A vs. 4A, difference in −2 log likelihood 465.7 − 448.9 = 16.8, 1 *df*, $P < 0.001$ χ^2 test with Bonferroni adjustment for nine possible comparisons between the five bivariate models in Table 3). Of these two models, the one that included MVD was the better predictor (model 5A vs. 3A, 448.9 − 438.7 = 10.2, 1 *df*, $P = 0.013$ with Bonferroni correction). The model that combined MLN with microvascular loops and networks was significantly better than those that combined MLN with ciliary body involvement and LBD (e.g., model 4A vs. 2A, 494.1 − 465.7 = 28.4, 1 *df*, $P < 0.001$ with Bonferroni correction).

When the four best predictors were combined in trivariate models (see Table 3 for models that included MVD), MLN lost statistical significance when modeled as a continuous variable ($P = 0.11$–0.18) but retained significance as a categorical one ($P = 0.023$–0.067). No model was notably better than the others. Combined in a single model, all four variables remained independent predictors of prognosis when MLN was modeled as a categorical variable ($P = 0.084$, model 8B), but as a continuous one, MLN was not statistically significant ($P = 0.28$, model 8A). Compared with the best trivariate models, the final models predicted survival significantly better (e.g., model 8B vs. 7B, 416.8 − 402.4 = 14.4, 1 *df*, $P < 0.001$; Bonferroni adjustment for three possible comparisons).

DISCUSSION

The mean MLN in this population-based, consecutive series of patients with primary choroidal and ciliary body melanoma was 3.71 to 4.06 μm, depending on the observer— on average, somewhat larger than in previous studies.[6–8,15,17] The range of observations, however, has been rather consistent between all studies.

Several factors affect mean MLN. Nucleoli measured in silver rather than hematoxylin-eosin–stained sections appear significantly larger.[17] The mean difference in one comparative series was 0.29 μm overall, and as high as 0.44 μm for patients who died of melanoma.[17] If the horizontal rather than the longest diameter of nucleoli is measured, obviously, MLN will be smaller.[15] When MLN is sampled from the entire tumor, the mean value is reported to be 0.15 μm larger than if a 5-mm linear field through tumor center is scanned.[17] Because MLN is associated with death from uveal melanoma,[2,5–7,10,15,17] enrollment criteria affect the mean value. Most previous studies were based on analysis of unconventional, selected data sets in which one half of patients died of melanoma and the other half survived for at least 10 years without metastasis,[2,4,7,17] or a variation thereof.[15] Because these analyses excluded patients who survived in the short term but were still at risk of dying of uveal melanoma, the mean MLN was probably biased toward

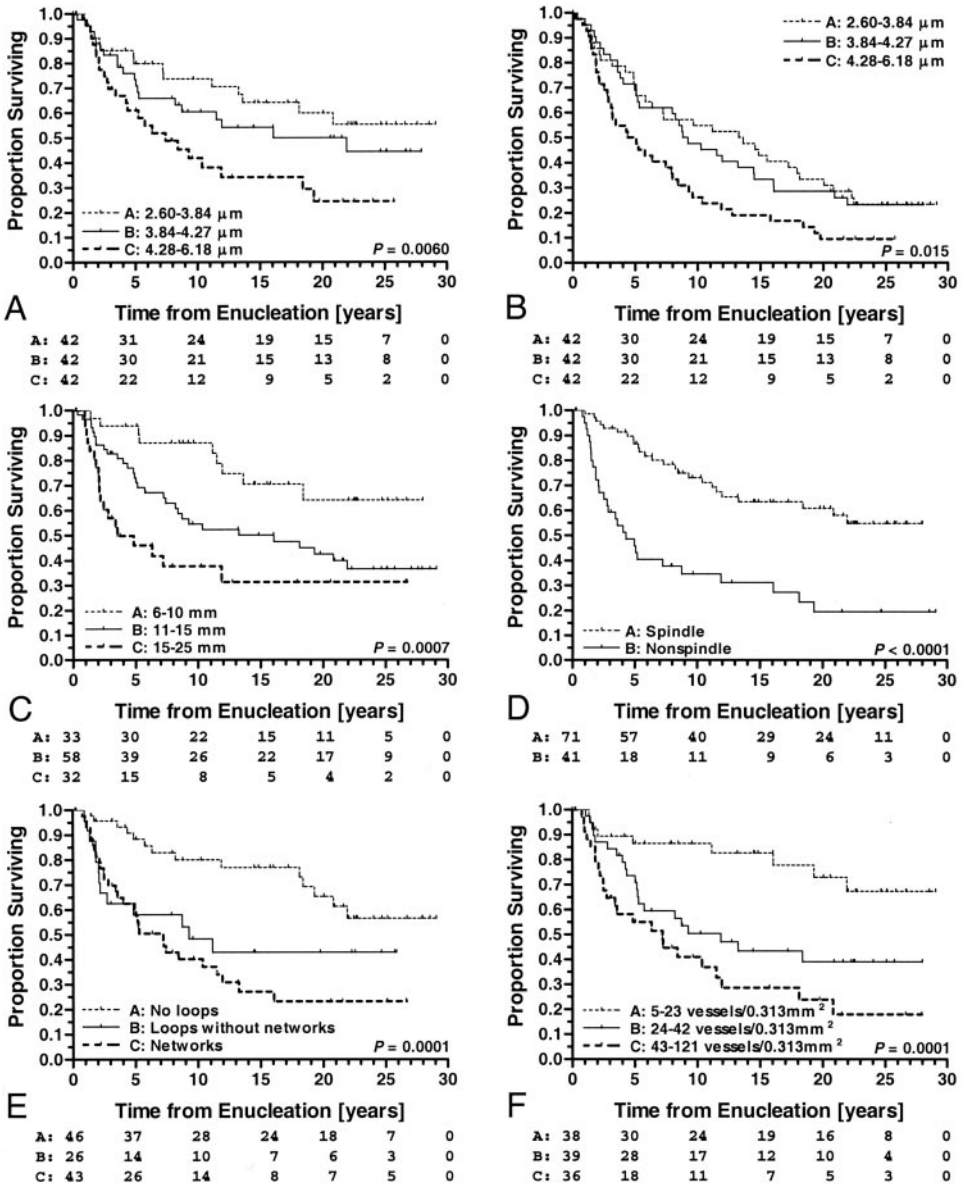

FIGURE 3. Melanoma-specific (**A**, **C**–**F**) and all-cause mortality (**B**) Kaplan-Meier survival curves for choroidal and ciliary body melanoma (*ticks*: censored observations). The melanoma-specific (**A**) and all-cause survival (**B**) of patients with large MLN was shorter than that of patients with small MLN. The LBD (**C**), presence of epithelioid cells (**D**), presence of microvascular loops and networks (**E**), and MVD obtained with antibodies against CD34 epitope from areas of highest vascularization (**F**) also differentiated patients with good and poor prognosis. *Numbers* below graphs show number of patients who remain in follow-up.

lower values. Finally, the measurements of one observer may be higher than those of another. One study found a mean difference of 0.20 μm,[8] and in our study it was 0.38 μm.

In addition to interobserver variation, use of a population-based data set and silver staining probably contributed to the larger than average mean MLN in our study. If differences in measuring remain consistent from specimen to specimen, they should not seriously affect the prognostic association of MLN. In our data set, MLN was significantly associated with death of uveal melanoma, and this result was not affected by interobserver variation in measuring MLN. The 10-year cumulative proportion of patients who died was 0.32 units larger if patients had a melanoma with a large rather than small MLN, and Cox regression estimated the risk of dying to be 3.1 times higher for the former group. In another consecutive series, the 10-year survival difference was estimated to be 0.47.[6]

With one exception, MLN has consistently been associated with melanoma-specific mortality by univariate analysis.[2,4,7,10,17] For each 1-μm change, the regression coefficient has ranged from 0.58 to 1.27.[2,4,7,10,17] Our estimate falls within this range. Most previous estimates were based on the selected data sets mentioned earlier herein,[2,4,7,15,17] which may have introduced bias in estimating effect size and in hypothesis testing.

MLN was significantly higher in melanomas that contained epithelioid cells,[15,17] and we found no significant difference in MLN according to ciliary body involvement[15] and presence of microvascular loops and networks,[8,15] as previously reported. MLN was not significantly associated with LBD, in contrast to previous reports that found a weak to moderate correlation.[8,15,17] A new finding was that MLN correlated positively with MVD.

Despite the association between MLN and presence of epithelioid cells, both independently predicted survival by bivariate Cox regression, confirming some[5] but not all previous analyses.[2] Moreover, this model fitted significantly better to the data than competing ones that included ciliary body involvement, LBD, and microvascular loops and networks. Our findings that MLN retained significance when adjusting for LBD,[2,4,5] loops,[10] and networks[15] are in line with previous multivariate studies. It is consequently well established that MLN and microvascular loops and networks in uveal melanoma are unrelated, but other microvascular patterns have not been evaluated in this regard.

TABLE 3. Multivariate Modeling of Melanoma-Specific Survival of Patients with 126 Choroidal and Ciliary Body Melanomas

	MLN Modeled as a Continuous Variable				MLN Modeled as a Categorical Variable			
	Regression Coefficient (SE)	Wald χ^2	*P*	HR (95% CI)	Regression Coefficient (SE)	Wald χ^2	*P*	HR (95% CI)
Univariate Analysis								
MLN	0.600 (0.249)	5.85	0.016	1.82 (1.12–2.97)	0.449 (0.166)	7.34	0.007	1.57 (1.13–2.17)
Gender*	0.319 (0.268)	1.42	0.24	1.38 (0.81–2.33)	Not applicable			
Tumor location†	0.849 (0.287)	8.82	0.003	2.34 (1.33–4.09)	Not applicable			
Largest basal diameter‡	0.110 (0.035)	12.0	0.001	1.13 (1.05–1.20)	Not applicable			
Cell type§	0.825 (0.216)	14.7	<0.001	2.28 (1.50–3.48)	Not applicable			
Pigmentation‖	0.432 (0.181)	5.71	0.017	1.54 (1.08–2.20)	Not applicable			
Microvascular pattern¶	0.587 (0.157)	14.1	<0.001	1.80 (1.32–2.44)	Not applicable			
Microvascular density#	0.022 (0.005)	19.1	<0.001	1.02 (1.01–1.03)	Not applicable			
Bivariate Analysis								
	Model 1A, −2 log likelihood = 499.4				**Model 1B, −2 log likelihood = 498.44**			
MLN	0.501 (0.251)	4.00	0.046	1.65 (1.00–2.70)	0.371 (0.167)	4.92	0.026	1.45 (1.04–2.01)
Tumor location†	0.775 (0.288)	7.23	0.007	2.17 (1.23–3.81)	0.743 (0.289)	6.60	0.010	2.10 (1.19–3.71)
	Model 2A, −2 log likelihood = 494.1				**Model 2B, −2 log likelihood = 492.9**			
MLN	0.537 (0.260)	4.24	0.039	1.71 (1.03–2.85)	0.386 (0.167)	5.29	0.022	1.47 (1.06–2.05)
Largest basal diameter‡	0.121 (0.035)	11.7	0.001	1.13 (1.05–1.21)	0.118 (0.356)	11.0	0.001	1.13 (1.05–1.20)
	Model 3A, −2 log likelihood = 448.9				**Model 3B, −2 log likelihood = 446.7**			
MLN	0.681 (0.269)	6.40	0.011	1.98 (1.16–3.35)	0.507 (0.177)	8.24	0.004	1.66 (1.17–2.35)
Cell type§	0.907 (0.232)	15.3	<0.001	2.48 (1.57–3.90)	0.904 (0.228)	15.7	<0.001	2.48 (1.58–3.87)
	Model 4A, −2 log likelihood = 465.7				**Model 4B, −2 log likelihood = 464.12**			
MLN	0.569 (0.287)	3.92	0.048	1.77 (1.00–3.10)	0.412 (0.177)	5.42	0.020	1.51 (1.07–2.14)
Microvascular patterns¶	0.596 (0.158)	14.4	<0.001	1.81 (1.33–2.47)	0.593 (0.158)	14.0	<0.001	1.80 (1.32–2.46)
	Model 5A, −2 log likelihood = 438.7				**Model 5B, −2 log likelihood = 435.49**			
MLN	0.416 (0.258)	2.59	0.11	1.51 (0.91–2.51)	0.319 (0.172)	3.42	0.064	1.37 (0.98–1.93)
Microvascular density#	0.021 (0.005)	16.6	<0.001	1.02 (1.01–1.03)	0.304 (0.075)	16.4	<0.001	1.35 (1.17–1.57)
Multivariate Analysis								
	Model 6A, −2 log likelihood = 421.5				**Model 6B, −2 log likelihood = 417.85**			
MLN	0.374 (0.276)	1.82	0.18	1.45 (0.84–2.50)	0.323 (0.176)	3.34	0.067	1.38 (0.98–1.95)
Cell type§	1.098 (0.254)	18.6	<0.001	3.00 (1.82–4.94)	1.108 (0.254)	19.0	<0.001	3.02 (1.84–4.99)
Microvascular density#	0.021 (0.005)	17.1	<0.001	1.02 (1.01–1.03)	0.309 (0.077)	16.2	<0.001	1.36 (1.17–1.58)
	Model 7A, −2 log likelihood = 418.0				**Model 7B, −2 log likelihood = 416.79**			
MLN	0.434 (0.284)	2.34	0.13	1.54 (0.89–2.70)	0.334 (0.180)	3.45	0.063	1.39 (0.98–1.99)
Microvascular patterns¶	0.496 (0.162)	9.30	0.002	1.64 (1.19–2.26)	0.493 (0.163)	9.12	0.002	1.64 (1.19–2.26)
Microvascular density#	0.283 (0.800)	12.5	<0.001	1.33 (1.13–1.56)	0.279 (0.080)	12.0	0.001	1.32 (1.13–1.55)
	Model 8A, −2 log likelihood = 404.3				**Model 8B, −2 log likelihood = 402.4**			
MLN	0.316 (0.291)	1.18	0.28	1.37 (0.78–2.42)	0.313 (0.181)	2.99	0.084	1.36 (0.95–1.95)
Cell type§	1.058 (0.281)	14.1	<0.001	2.88 (1.66–5.00)	1.083 (0.283)	14.7	<0.001	2.95 (1.69–5.13)
Microvascular patterns¶	0.360 (0.169)	4.58	0.032	1.43 (1.03–2.00)	0.361 (0.169)	4.53	0.033	1.43 (1.02–2.00)
Microvascular density#	0.291 (0.080)	13.4	<0.001	1.33 (1.14–1.57)	0.284 (0.080)	12.5	<0.001	1.32 (1.13–1.55)

* Coding: Male, 0; Female, 1.
† Coding: Choroid only, 0; Ciliary body involved, 1.
‡ Continuous variable, mm.
§ Coding: Spindle, 0; Nonspindle (epithelioid and mixed), 1.
‖ Coding: Weak, 0; Moderate, 1; Strong, 2.
¶ Coding: No loops, 0; Loops without networks, 1; Networks, 2.
# Continuous variable, square-root transformed vessel count/0.313 mm^2.

MVD is emerging as an important prognostic indicator that is independent of microvascular loops and networks in uveal melanoma.[28,31,35] It is evaluated by antibodies to endothelial cell markers—in particular, factor VIII-related antigen[26,28,31] and the CD34 epitope.[31,35] It is not known for certain whether all elements labeled with these antibodies, particularly CD34, are truly endothelial cells.[31] Evidence has been provided that a population of uveal melanoma cells may be immunopositive, suggesting a theory that the association of MVD with prognosis may, at least in part, reflect presence of more aggressive tumor cells that share features with endothelial ones.[35]

When MLN and MVD were entered into a bivariate Cox model as continuous variables, the independent association of MLN with survival weakened, but the fit of the model significantly improved, compared with competing models. The fit further improved if multivariate models that additionally included microvascular loops and networks and epithelioid cells were constructed, with further erosion in the independent prognostic significance of MLN. However, if divided in tertiles and modeled as a categorical variable, MLN retained independent association with prognosis in multivariate models. The difference may in part depend on the relatively small sample size.

That microvascular factors and nucleolar size independently predicted prognosis in uveal melanoma is consistent with a hypothesis that they represent, to a significant extent, different processes or stages that contribute to metastatic efficiency, such as the ability to invade and seed metastases and the ability to proliferate. In addition to reflecting aggressiveness of uveal melanoma cells,[33] loops, networks, and hot spots that contribute to high MVD harbor vascular channels that may directly be involved when melanoma cells enter the blood circulation. It could be postulated that nucleolar size is associated with tumor growth rate, given that high metabolic activity is linked with

active transcription, translation, and gene activation. The ability to seed metastasis and to proliferate are likely to be interrelated,[36] and we observed that MVD explains some of the prognostic association of MLN. Because uveal melanoma cells sometimes seem to express antigens on which measurement of MVD is based,[35] one could assess nucleoli in tumors suspected of containing cells that share these antigens to look for a relationship at the cellular level.

In conclusion, using an independent population-based data set, we were not only able to confirm that MLN and microvascular loops and networks are unrelated, independent predictors of survival in uveal melanoma,[10,15] but we also found that multivariate models that include MVD in addition to MLN fit significantly better with survival data than models that exclude MVD. Although noninvasive detection of microvascular factors is now technically possible[36,48,49] and a desirable and significant step forward in managing patients with uveal melanoma,[50] our study suggests that such noninvasive methods will not fully capture the process of clinical metastasis from the primary tumor. Progress in resection techniques is likely to provide in the near future fresh material for the ophthalmic pathologist to correlate angiographic data with genetic and histopathologic characteristics such as MLN.

References

1. Mikel UV, Engler WF, Perez-Rosario E, Becker RL, McLean IW. A comparative study of morphometric measurements of nucleoli in uveal melanomas from electron micrographs and plastic-embedded and paraffin-embedded sections. *Anal Quant Cytol Histol.* 1989;11:111–114.
2. Huntington A, Haugan P, Gamel J, McLean I. A simple cytologic method for predicting the malignant potential of intraocular melanoma. *Pathol Res Pract.* 1989;185:631–634.
3. Marcus DM, Minkovitz JB, Wardwell SD, Albert DM. The value of nucleolar organizer regions in uveal melanoma: The Collaborative Ocular Melanoma Study Group. *Am J Ophthalmol.* 1990;110:527–534.
4. McCurdy J, Gamel J, McLean I. A simple, efficient, and reproducible method for estimating the malignant potential of uveal melanoma from routine H & E slides. *Pathol Res Pract.* 1991;187:1025–1027.
5. Gamel JW, McCurdy JB, McLean IW. A comparison of prognostic covariates for uveal melanoma. *Invest Ophthalmol Vis Sci.* 1992; 33:1919–1922.
6. Sørensen FB, Gamel JW, Jensen OA, Ladekarl M, McCurdy J. Prognostic value of nucleolar size and size pleomorphism in choroidal melanomas. *APMIS.* 1993;101:358–368.
7. Sørensen FB, Gamel JW, McCurdy J. Stereologic estimation of nucleolar volume in ocular melanoma: a comparative study of size estimators with prognostic impact. *Hum Pathol.* 1993;24:513–518.
8. Pe'er J, Rummelt V, Mawn L, Hwang T, Woolson RF, Folberg R. Mean of the ten largest nucleoli, microcirculation architecture, and prognosis of ciliochoroidal melanomas. *Ophthalmology.* 1994; 101:1227–1235.
9. Rummelt V, Folberg R, Woolson RF, Hwang T, Pe'er J. Relation between the microcirculation architecture and the aggressive behavior of ciliary body melanomas. *Ophthalmology.* 1995;102:844–851.
10. McLean IW, Keefe KS, Burnier MN. Uveal melanoma: comparison of the prognostic value of fibrovascular loops, mean of the ten largest nucleoli, cell type, and tumor size. *Ophthalmology.* 1997; 104:777–780.
11. McLean IW, Sibug ME, Becker RL, McCurdy JB. Uveal melanoma: the importance of large nucleoli in predicting patient outcome: an automated image analysis study. *Cancer.* 1997;79:982–988.
12. Staibano S, Orabona P, Mezza E, et al. Morphometric analysis of AgNORs in uveal malignant melanoma. *Anal Quant Cytol Histol.* 1998;20:483–492.
13. Baldi G, Baldi F, Maguire M, Massaro-Giordano M. Prognostic factors for survival after enucleation for choroidal melanoma. *Int J Oncol.* 1998;13:1185–1189.
14. Tuccari G, Gimenez-Mas JA, Fedele F, et al. The AgNOR quantity as prognostic parameter in choroidal melanomas: a standardised analysis. *Anal Cell Pathol.* 1999;19:163–168.
15. Seregard S, Spångberg B, Juul C, Oskarsson M. Prognostic accuracy of the mean of the largest nucleoli, vascular patterns, and PC-10 in posterior uveal melanoma. *Ophthalmology.* 1998;105:485–491.
16. Tuccari G, Giuffrè G, Gimenez-Mas JA, Öfner D. Morphometric analysis of AgNORs in uveal malignant melanoma. *Anal Quant Cytol Histol.* 2000;22:183–184.
17. Moshari A, McLean IW. Uveal melanoma: mean of the longest nucleoli measured on silver-stained sections. *Invest Ophthalmol Vis Sci.* 2001;42:1160–1163.
18. Bardenstein DS, Char DH, Kaleta-Michaels S, Kroll SM. Ki-67 and bromodeoxyuridine labeling of human choroidal melanoma cells. *Curr Eye Res.* 1991;10:479–484.
19. Pe'er J, Gnessin H, Shargal Y, Livni N. PC-10 immunostaining of proliferating cell nuclear antigen in posterior uveal melanoma: enucleation versus enucleation postirradiation groups. *Ophthalmology.* 1994;101:56–62.
20. Seregard S, Oskarsson M, Spångberg B. PC-10 as a predictor of prognosis after antigen retrieval in posterior uveal melanoma. *Invest Ophthalmol Vis Sci.* 1996;37:1451–1458.
21. Pe'er J, Stefani FH, Seregard S, et al. Cell proliferation activity in posterior uveal melanoma after Ru-106 brachytherapy: an EORTC Ocular Oncology Group study. *Br J Ophthalmol.* 2001;85:1208–1212.
22. Folberg R, Pe'er J, Gruman LM, et al. The morphologic characteristics of tumor blood vessels as a marker of tumor progression in primary human uveal melanoma: a matched case-control study. *Hum Pathol.* 1992;23:1298–1305.
23. Chowers I, Folberg R, Livni N, Pe'er J. p53 Immunoreactivity, Ki-67 expression, and microcirculation patterns in melanoma of the iris, ciliary body, and choroid. *Curr Eye Res.* 2002;24:105–108.
24. Folberg R, Rummelt V, Parys-van Ginderdeuren R, et al. The prognostic value of tumor blood vessel morphology in primary uveal melanoma. *Ophthalmology.* 1993;100:1389–1398.
25. Rummelt V, Folberg R, Rummelt C, et al. Microcirculation architecture of melanocytic nevi and malignant melanomas of the ciliary body and choroid: a comparative histopathologic and ultrastructural study. *Ophthalmology.* 1994;101:718–727.
26. Foss AJE, Alexander RA, Jefferies LW, Hungerford JL, Harris AL, Lightman S. Microvessel count predicts survival in uveal melanoma. *Cancer Res.* 1996;56:2900–2903.
27. Schaling DF, Van der Pol JP, Schlingemann RO, Parys-van Ginderdeuren R, Ruiter DJ, Jager MJ. Vascular density and vascular patterns in the prognosis of choroidal melanoma. Thesis D. F. Schaling: *Radionuclides and Radiolabelled Antibodies in Choroidal Melanoma*: *Diagnosis and Therapy.* Leiden: Rijksuniversiteit te Leiden; 1996:43–54.
28. Foss AJE, Alexander RA, Hungerford JL, Harris AL, Cree IA, Lightman S. Reassessment of the PAS patterns in uveal melanoma. *Br J Ophthalmol.* 1997;81:240–246.
29. Lane AM, Egan KM, Yang J, et al. An evaluation of tumour vascularity as a prognostic indicator in uveal melanoma. *Melanoma Res.* 1997;7:237–242.
30. Mehaffey MG, Folberg R, Meyer M, et al. Relative importance of quantifying area and vascular patterns in uveal melanomas. *Am J Ophthalmol.* 1997;123:798–809.
31. Mäkitie T, Summanen P, Tarkkanen A, Kivelä T. Microvascular density in predicting survival of patients with choroidal and ciliary body melanoma. *Invest Ophthalmol Vis Sci.* 1999;40:2471–2480.
32. Mäkitie T, Summanen P, Tarkkanen A, Kivelä T. Microvascular loops and networks as prognostic indicators in choroidal and ciliary body melanomas. *J Natl Cancer Inst.* 1999;91:359–367.
33. Maniotis AJ, Folberg R, Hess A, et al. Vascular channel formation by human melanoma cells in vivo and in vitro: vasculogenic mimicry. *Am J Pathol.* 1999;155:739–752.
34. Folberg R, Chen X, Boldt HC, et al. Microcirculation patterns other than loops and networks in choroidal and ciliary body melanomas. *Ophthalmology.* 2001;108:996–1001.

35. Chen X, Maniotis AJ, Majumdar D, Pe'er J, Folberg R. Uveal melanoma cell staining for CD34 and assessment of tumor vascularity. *Invest Ophthalmol Vis Sci.* 2002;43:2533–2539.
36. Folberg R, Hendrix MJC, Maniotis AJ. Vasculogenic mimicry and tumor angiogenesis. *Am J Pathol.* 2000;156:361–381.
37. Damato B. Adjunctive plaque radiotherapy after local resection of uveal melanoma. *Front Radiat Ther Oncol.* 1997;30:123–132.
38. Damato B, Groenewald CP, McGalliard JN, Wong D. Rhegmatogenous retinal detachment after transscleral local resection of choroidal melanoma. *Ophthalmology.* 2002;109:2137–2143.
39. Bechrakis NE, Bornfeld N, Zoller I, Foerster MH. Iodine 125 plaque brachytherapy versus transscleral tumor resection in the treatment of large uveal melanomas. *Ophthalmology.* 2002;109:1855–1861.
40. Mäkitie T, Summanen P, Tarkkanen A, Kivelä T. Tumor-infiltrating macrophages ($CD68^+$ cells) and prognosis in malignant uveal melanoma. *Invest Ophthalmol Vis Sci.* 2001;42:1414–1421.
41. Fuchs U, Kivelä T, Summanen P, Immonen I, Tarkkanen A. An immunohistochemical and prognostic analysis of cytokeratin expression in malignant uveal melanoma. *Am J Pathol.* 1992;141: 169–181.
42. Ramani P, Bradley NJ, Fletcher CDM. QBEND/10, a new monoclonal antibody to endothelium: assessment of its diagnostic utility in paraffin sections. *Histopathology.* 1990;17:237–242.
43. Altman DG. *Practical Statistics for Medical Research.* London: Chapman & Hall; 1991.
44. Cuzick J. A Wilcoxon-type test for trend. *Stat Med.* 1985;4:87–90.
45. Parmar MKB, Machin D. *Survival Analysis. A Practical Approach.* Chichester, UK: John Wiley & Sons; 1996.
46. Hosmer DW Jr, Lemeshow S. *Applied Survival Analysis*: *Regression Modeling of Time to Event Data.* New York: John Wiley & Sons; 1999.
47. Therneau TM, Grambsch PM. *Modeling Survival Data: Extending the Cox Model.* New York: Springer; 2000.
48. Silverman RH, Folberg R, Boldt HC, et al. Correlation of ultrasound parameter imaging with microcirculatory patterns in uveal melanomas. *Ultrasound Med Biol.* 1997;23:573–581.
49. Mueller AJ, Bartsch DU, Folberg R, et al. Imaging the microvasculature of choroidal melanomas with confocal indocyanine green scanning laser ophthalmoscopy. *Arch Ophthalmol.* 1998;116:31–39.
50. Mueller AJ, Freeman WR, Schaller UC, Kampik A, Folberg R. Complex microcirculation patterns detected by confocal indocyanine green angiography predict time to growth of small choroidal melanocytic tumors: MuSIC Report II. *Ophthalmology.* 2002;109: 2207–2214.